

Optical chromatographic sample separation of hydrodynamically focused mixtures

A. Terray,^{1,a)} C. G. Hebert,¹ and S. J. Hart²

¹*Bio/Analytical Chemistry, Chemistry Division, Naval Research Laboratory, Code 6112, 4555 Overlook Ave. S.W., Washington, District of Columbia 20375, USA*

²*LumaCyte, 3966 Stony Point Road, Keswick, Virginia 22947, USA*

(Received 29 September 2014; accepted 4 November 2014; published online 11 November 2014)

Optical chromatography relies on the balance between the opposing optical and fluid drag forces acting on a particle. A typical configuration involves a loosely focused laser directly counter to the flow of particle-laden fluid passing through a microfluidic device. This equilibrium depends on the intrinsic properties of the particle, including size, shape, and refractive index. As such, uniquely fine separations are possible using this technique. Here, we demonstrate how matching the diameter of a microfluidic flow channel to that of the focusing laser in concert with a unique microfluidic platform can be used as a method to fractionate closely related particles in a mixed sample. This microfluidic network allows for a monodisperse sample of both polystyrene and poly(methyl methacrylate) spheres to be injected, hydrodynamically focused, and completely separated. To test the limit of separation, a mixed polystyrene sample containing two particles varying in diameter by less than 0.5 μm was run in the system. The analysis of the resulting separation sets the framework for continued work to perform ultra-fine separations.

© 2014 AIP Publishing LLC. [<http://dx.doi.org/10.1063/1.4901824>]

I. INTRODUCTION

The optical manipulation of microscopic particles via laser radiation has become an established area of research with links to a wide variety of research communities including but not limited to the chemical, biological, and medical fields.^{1–6} In all cases, photon wavelength and density are manipulated to directly influence the forces resulting from the momentum exchange of photons refracting through and reflecting off of the microscopic samples of interest.⁷ The creative control and direction of these forces have been used to trap, manipulate, and separate a variety of microscopic particle types.⁵ In one such application, optical tweezers or optical trapping employ one or more highly focused laser radiation sources to manipulate a sample.⁷ Although it depends on whether the sample is suspended in a fluid of lower or higher refractive index than the particle of interest, highly convergent Gaussian laser radiation is typically used. In the case of a liquid with a lower refractive index than the sample, the resulting dominant gradient force retains particles at the focal point of the converging rays. Once trapped, individual, and multi-particle translations and manipulations have been achieved through the translation of the fluid, flowcell, or laser beam.^{8–10} Successful separation of microscopic particles based on their appearance has also been achieved,¹¹ while more recent work has utilized arrays of optical traps to separate particles based upon their intrinsic optical mobilities.⁸ Other techniques involve manipulating the incident laser beam to separate samples.¹²

Optical chromatography^{13,14} deviates from optical tweezers in that it relies on a mildly focused laser beam to interrogate or manipulate particles. In this case, the Gaussian nature of the beam results in a gradient optical force that draws particles into the beam while the dominant scattering force propels them along the direction of laser propagation. In practice, the laser

^{a)} Author to whom correspondence should be addressed. Electronic mail: terray@nrl.navy.mil.

radiation is focused directly opposing fluid flow and trapped particles are held where the fluid drag and combined optical pressure forces are equal. Particles that are larger in size and/or have a greater refractive index, experience greater optical forces and are thus retained further from the focal point of the laser than smaller or lower refractive index particles. This retention distance is unique for a particle and depends on the particles intrinsic properties such as size, shape and composition. Using this technique, it has been shown that particles and biological samples can be separated by size,^{14,15} refractive index,¹⁶ shape and morphology,¹⁷ and fluid drag characteristics.¹⁷ It has even been shown that with multiple lasers and a complex microfluidic design, multi-component biological samples can be fractionated.¹⁸

In this paper, we expand on our previous work by improving the separation capability of the system through the development of a novel “trap and release” technique. By first hydrodynamically focusing an injected sample before it encounters the separation laser, we are able to reproducibly and completely separate a sample that was previously poorly separated. In recent optical chromatography research,^{13–17} a lightly focused laser has been used to fractionate, concentrate, and/or collect the sample.^{19,20} The goal with this new implementation of optical chromatography is to perform complete separation of sample mixtures containing similar particle types, which were previously unsuccessful. While a number of methods have been demonstrated to analyze particles and cells in microfluidic systems without the use of labels,^{21–23} the added ability to fractionate and/or purify a sample on-chip that can ultimately be collected off-chip in a facile manner²⁰ can be advantageous for integration with existing technologies that require sample cleanup as well as the development of new techniques for the separation of highly similar species.

II. EXPERIMENTAL

The device discussed here consisted of a fluidic system including all liquid handling, with pumping and injections, coupled with an optical apparatus. The combined result included three independently controllable Continuous Wave (CW) 1064-nm ytterbium fiber lasers (IPG Photonics, Oxford, MA, USA) focused into the fused silica microfluidic device, although only two were used in the work presented here. The lasers were each focused into the microfluidic system by a 0.5 in. diameter plano-convex 100 mm focal length lens. The microfluidic flowcell was mounted on a 5 axis positioner (New Focus, San Jose, CA, USA), and the entire aligned optic and fluidic system was observed using a 20 \times objective and lens tube system (Infinity Photo-Optical, Boulder, CO, USA) connected to a Charge-Coupled Device (CCD) camera (Olympus America, Inc., Center Valley, PA, USA) mounted independent of the optic and fluidic components.

The microfluidic flowcell, similar in construction to previous work,¹⁸ shown in Figure 1, consisted of three plates of fused silica. The 250 μm thick center plate was wet etched in hydrofluoric acid (HF) to yield a structure of etched trenches, 85 μm wide and 40–70 μm deep, on both sides of the plate with several 50 μm diameter capillary thru-holes connecting the trenches on either side of the plate (Translume Inc, Ann Arbor, MI, USA). This layer was bonded between two 2 mm thick outer plates at room temperature²⁴ into which was drilled a 350 μm diameter hole that aligned with the injection channel on the central layer. The inlet and outlet channels extended to the edge of the chip and were accessed there. The bonded device was shaped and polished using a diamond lapping machine (Crystalite Corp., Westerville, OH, USA). Fluid connectors (Nanoport, Upchurch Scientific, Inc., Oak Harbor, WA) were epoxied to the finished chip to allow for fluid inlet, outlet, and injection tubing.

The fluid control system consisted of a pressure controlled volume of air over 20 ml of pure water. The liquid volume was connected to tubing and by precisely manipulating the pressure in the air volume, pulseless, stable, and reproducible fluid flow was achieved. Computer control via an electronic pressure controller (OEM-EP, Parker Hannifin, Hollis, NH) allowed for rapid and interactive manipulation of the pressure and, therefore, flow rate. The complete system involved connecting the inlet and outlet tubing to separate reservoirs. The dual reservoir technique isolated the flow system, increasing the stability, and added the ability to control

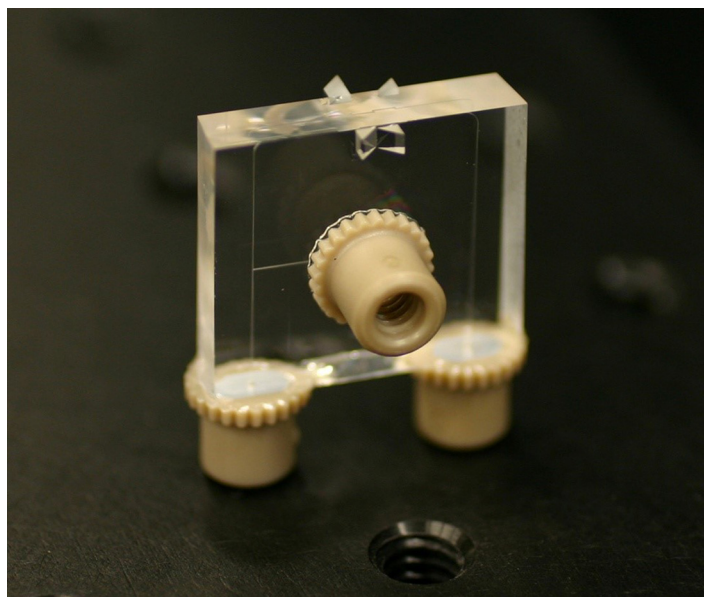


FIG. 1. Optical chromatography separation flowcell. The inlet, outlet, and injection channels can be seen in the three layer fused silica device. The prisms allow for up to three lasers to be directed into three separation regions.

flow direction. Flow direction and flow rate were precisely measured to a resolution of 0.5 nl/min using a calibrated commercial liquid mass flow meter (Sensirion Inc., Westlake Village, CA, USA).

Sample injections were made using a syringe pump (NE-1000, New Era Pump Systems Inc, Farmingdale, NY) fitted with a 10 μ l syringe (Hamilton, Reno, NV, USA). The two mixture samples consisted of two components each, with the first containing: 2.74 μ m (StDev = 0.05 μ m) polystyrene (PS) spheres ($n = 1.59$), and 2.74 μ m (StDev = 0.04 μ m) poly(methyl methacrylate) (PMMA) spheres ($n = 1.49$) (microParticles GmbH, Berlin, Germany) and the second mixture containing: 2.74 μ m and 2.39 μ m (StDev = 0.04 μ m) PS spheres (microParticles GmbH, Berlin, Germany).

For each injection, a novel method to focus the sample in three-dimensions was employed and is shown in Figure 2. Utilizing a single defocused laser at high power (8 W), an entire injected sample of mixed particles was optically collected from the flow and concentrated against the microfluidic wall. The concentrated mound of particles was then released by using a computer control program to slowly and reproducibly reduce the power of the laser holding them in place. As this occurred, particles were focused and drawn individually into the surrounding flow field, into the 50 μ m capillary and out to the next separation region. Due to the microfluidic pathway that incorporated an increase in the channel width or “frying pan” just before a 50 μ m capillary constriction, a flow field reminiscent of a three-dimensional hydrodynamic focusing nozzle was created. This flow field was responsible for pulling particles one at a time from the peak of the mound on the wall into a very reproducible three-dimensional position in the flow. Because the laser used to constrain the particles was defocused and spread across a wide area, the gradient forces were negligible. This method was truly hydrodynamic as the laser only acted as a mediator, regulating the rate with which particles entered the hydrodynamic focusing region while having no effect on the particle focusing itself.

Hydrodynamically focused particles continued horizontally 250 μ m through the focusing region and another 500 μ m downward until they reached the separation region shown in Figure 3. At this point, particles encountered the laser and were either held against the wall or allowed to continue to enter the 50 μ m capillary. The separation occurred as particles in the flow were making the 90° turn into the capillary. For each experiment, a pure injection of each particle type making up the mixture was injected for identification, focus verification, and separation optimization. Minimal adjustment of the objective focal plane was required to maintain

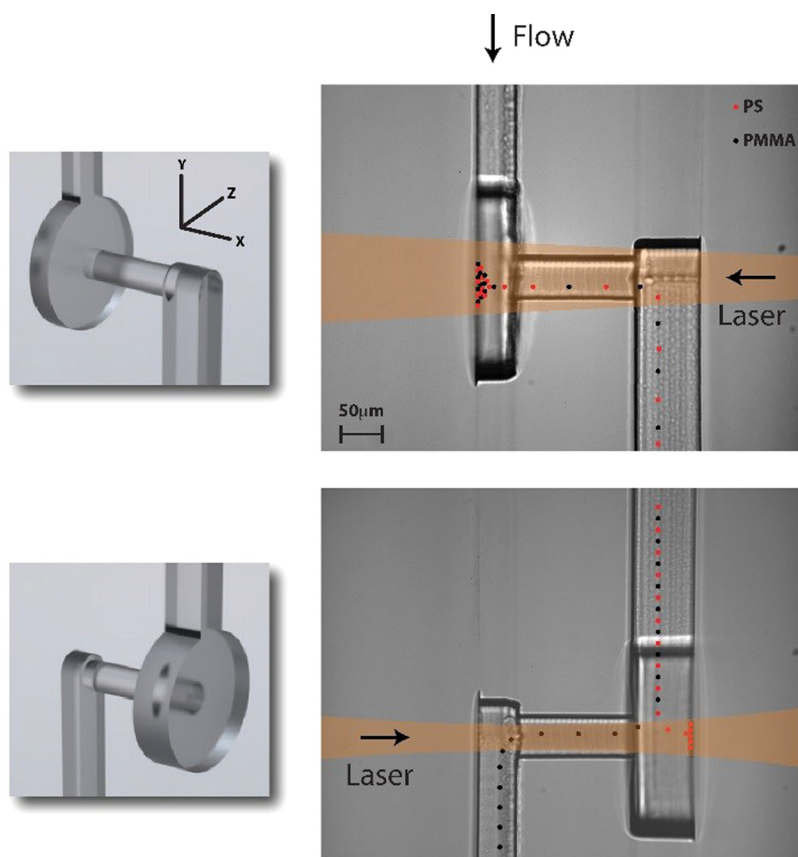


FIG. 2. An illustration showing both the hydrodynamic focusing (top) and separation regions (bottom) within the vertical flowcell. Red and black dots illustrate common particle trajectories. The overlay images on the left show the “frying pan” region just before the $50\ \mu\text{m}$ capillary in both regions. Particles were collected and released in a focused stream in the top region and perfectly separated before the $50\ \mu\text{m}$ capillary in the bottom region.

particle focus within the image, thus verifying the consistency of particle position in and out of the viewing plane. For a specific flow rate, the laser power was adjusted to map out the entire range from complete trapping to no trapping for each sample. With this information, a laser power and flow rate were determined to give the separation the greatest possibility of success.

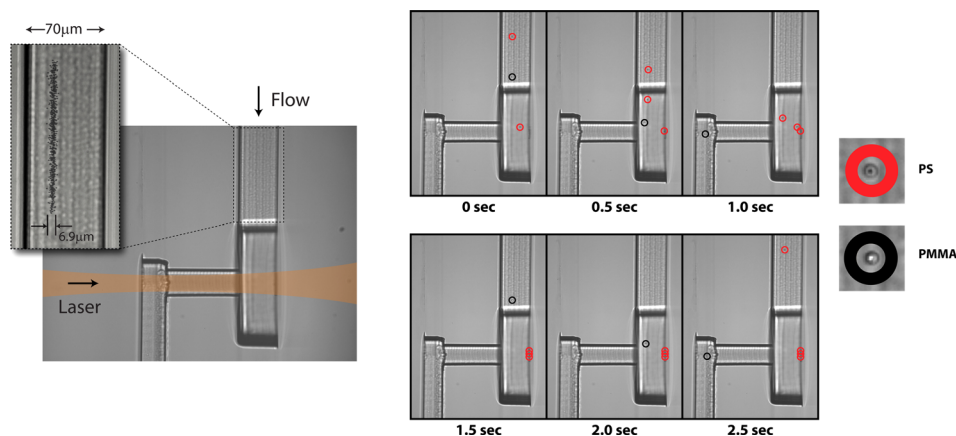


FIG. 3. Complete fractionation of $2.74\ \mu\text{m}$ PS and PMMA at $50\ \text{nl/min}$ with $3.1\ \text{W}$ of $1064\ \text{nm}$ laser power. The red and black circles are included to highlight the path and point of separation as the particles are drawn into the $50\ \mu\text{m}$ capillary and separated. The overlay image to the left shows the width of the focused particle stream by plotting the particle center data for an entire injection over the channel image.

Mixture samples were then injected, hydrodynamically focused, and separated. Particle identification and trajectories were subsequently analyzed.

Data collection and analysis were performed using ImagePro Plus version 6.2 (Media Cybernetics, Inc., Silver Spring, MD). Particles were counted both manually and using particle tracking routines within the software. For several replicate injections, particle center positions were tracked in software. Particle release from the wall was regulated such that particles traveled single file with space between each to remove particle-particle interactions and to aid in particle tracking. Because PS and PMMA have different refractive indices, the microscope image of each particle was visually different as each focuses the illumination differently. This is shown in Figure 3 where the PS, surrounded by the red circle, has a primarily black center and the PMMA, surrounded by the black circle, has a white center. Because particles were focused in the flow and were imaged at the same position, this was a reliable method to discriminate between PS and PMMA using automated analysis. For the $2.74\text{ }\mu\text{m}$ and $2.39\text{ }\mu\text{m}$ PS, this method also worked, but required an adjustment of focus such that the $2.74\text{ }\mu\text{m}$ PS particles had a light center and the $2.39\text{ }\mu\text{m}$ PS particles had a dark center. In this case, tracking was more difficult and was verified manually. In the case of manual tracking, a particle trajectory was followed to determine if it was retained or passed through the separation region. These data allowed for a full analysis of each separation.

III. RESULTS AND DISCUSSION

In a previous separation,¹⁸ we used the same device but relied on particles in flow that were separated regardless of their position in the flow. This method was used successfully for several different samples including the cleanup of biological samples for PCR.²⁰ As shown elsewhere, these separated samples can be individually collected outside the system for verification and use in other systems. With the success of these separations, there is always a desire to improve the resolution. A simulation study of our system suggested that a focused stream of particles would increase our separation resolution significantly.²⁵ To that end, we developed the current two laser system. Two sample mixtures were run. Each sample was a two component mixture with the first consisting of two chemically different but identically sized microspheres of PS and PMMA and the second involved two chemically identical but differently sized microspheres of PS.

Our first sample demonstrated the ability of our system to fractionate a previously difficult sample. This mixture sample contained $2.74\text{ }\mu\text{m}$ PS and PMMA particles in equal numbers. The separation was performed at a flow rate of 50 nl/min with a separation laser power of 3.1 W . The dispersion width of the focused particles in the channel before the separation was $6.9\text{ }\mu\text{m}$, shown in Figure 3. This width encompassed 95% of the particles and was calculated as two standard deviations from the average particle position in the channel over four separate injections totaling 2467 particles. The separations investigated here were batch in nature but if operated continuously would have resulted in a throughput of about 1.0 particle per second. Particle center data for one injection is shown in the overlay of Figure 3. When a similar separation was attempted using the previous method that lacked hydrodynamic focusing, the sample was poorly separated, yielding two samples that were 60%–70% pure in each separated component.¹⁸ In the current experiment, the mixed sample was hydrodynamically focused prior to separation, resulting in two 100% separated component streams. In replicate runs, the separation remained consistent and was not affected by the occasional doublet or triplet that occurred if the rate of particle release from the wall was increased. No cross component aggregates were observed. This result represents a significant improvement from our previous work. It is important to note that this separation does not just represent particles that are only retained or unreleased; they could easily be collected and removed from the system as two distinct pure samples. Furthermore, the entire injected stream (hydrodynamically released from the wall) was processed and separated at this efficiency.

To test the ability of our system to separate an even more difficult sample, a roughly equal number mixture of $2.74\text{ }\mu\text{m}$ and $2.39\text{ }\mu\text{m}$ PS was injected. With a flow rate of 50 nl/min , a

separation laser power of 2.6 W, and a focus width of $7.2\ \mu\text{m}$, the resulting separation yielded an average purity of 79% for the $2.74\ \mu\text{m}$ fraction and 70% for the $2.39\ \mu\text{m}$ fraction. This represents an improvement from the injected mixture but far from a perfect separation. Under further investigation, we were able to gain more insight into the separation. In Figure 4, the particle center data for an injection are plotted. Since the position, identity, and retention status of each particle were known, analysis of each particle's focusing position could be conducted in order to determine if improving the focusing of our sample could improve this separation. Using the individual position values across the channel, we grouped each particle into one of five bins spanning two standard deviations from the average to account for 95% of the sample. Looking at the complete sample spread across all five bins showed that in bins a–d, the $2.39\ \mu\text{m}$ PS particles were not retained, but 67% were retained in bin e. The corresponding $2.74\ \mu\text{m}$ sample yielded complete retention of particles in bins d and e, but only 0%, 27%, and 47% in bins a–c, respectively. When combined, this implies that if particles were spatially restricted to bin d, a complete 100% separation would be possible. The current focus width of $7.2\ \mu\text{m}$ for this sample would need to be reduced to $1.4\ \mu\text{m}$ and either an adjustment to the position, laser power or flow rate would need to be made. The overlay image in Figure 4 shows four particles and their location in the focused stream with the bottom two illustrating the position limits for a sample capable of 100% fractionation in our system. Current work to modify our microfluidic device capability to restrict particles to a stream with a width at or below $1.4\ \mu\text{m}$ is currently underway. As stage one of our device acts to focus particles by mediating their introduction from a mound near the wall at the point where flow passes through a constriction, it is a form of hydrodynamic focusing. The factors that influence the focus width in our system are flow

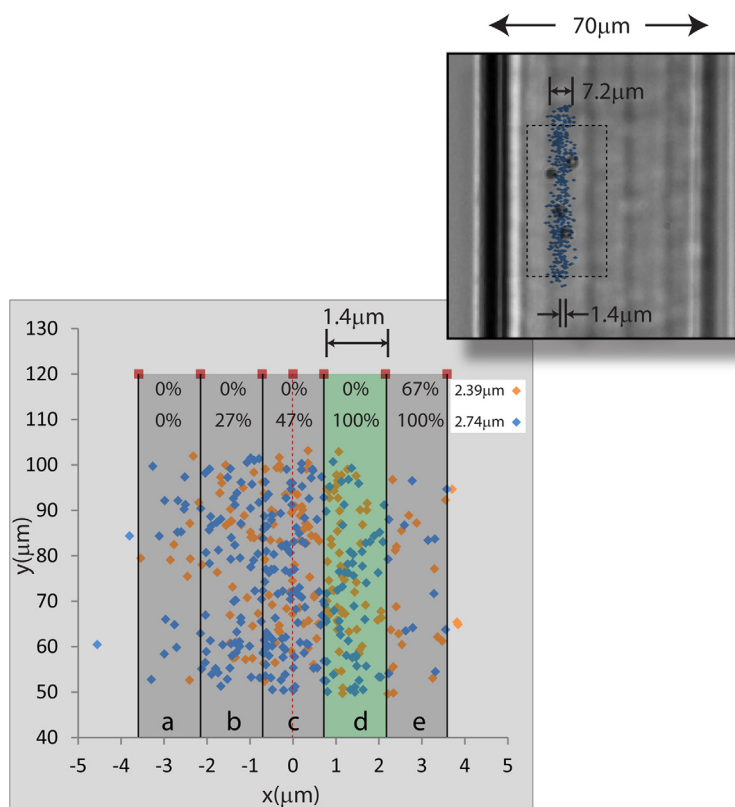


FIG. 4. Data from the fractionation of $2.74\ \mu\text{m}$ PS and $2.39\ \mu\text{m}$ PS. The plot shows center positions for a complete injection. The particle x-positions are divided into five bins a–e placed within two standard deviations of the average (indicated by the dotted red line). Within bin d, all particles are perfectly separated. In the overlay image the center data are plotted over actual particles from the injection. The top two particles occupy positions defining the overall width of the focused stream of particles where the bottom two occupy positions defining the width needed to achieve a complete separation.

rate, release rate from stage one and the distance the particles travel from the hydrodynamic focusing point. If we increase the flow rate, decrease the optically mediated release rate and shorten the distance to the separation stage, a decrease in the focus width would be expected, although an increase in flow would necessitate an increase in the power of the separation laser. Typically, a focused stream width is tightened in hydrodynamic focusing by increasing the ratio between the sheath and the core flow rates. Incorporation of a hydrodynamic focusing nozzle with a high sheath to core flow rate ratio would improve the stream width. Other forces, such as inertial, acoustic, magnetic, or electrophoretic, could also be used to achieve improved focusing.

It is interesting to note that, depending upon the particle composition, some rough separation did occur as particles were released from the wall in the top channel. As can be seen in Figure 5, the optically mediated release of particles in the first stage from the mound on the wall had an effect on the order in which they were focused into the flow. In the case of the $2.74\text{ }\mu\text{m}$ PS and PMMA mixture, Figure 5(a), the majority of the PMMA particles were released before the PS particles. In the case of the 2.39 and $2.74\text{ }\mu\text{m}$ PS mixture, Figure 5(b), the particles left the wall well mixed with no quantifiable preference, demonstrating the necessity of the second stage of the separation method. To better understand this result, we numerically estimated the optical scatter force for each of the particles in both mixtures,¹⁴ (5.97 pN for the $2.74\text{ }\mu\text{m}$ PS, 4.55 pN for the $2.39\text{ }\mu\text{m}$ PS and 3.17 pN for the $2.74\text{ }\mu\text{m}$ PMMA). It was found that the difference in optical force for the $2.74\text{ }\mu\text{m}$ PS and PMMA mixture was about twice that of the 2.39 and $2.74\text{ }\mu\text{m}$ PS mixture. Our numerical calculation assumes a single particle centered along the laser beam axis and does not account for the complex inter-particle physical,

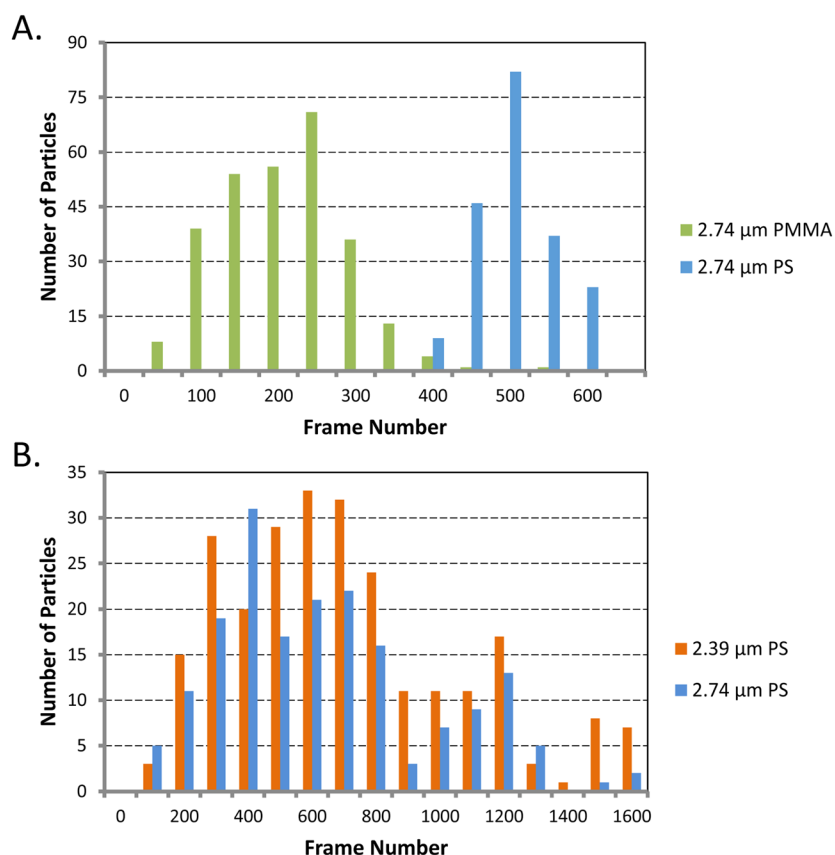


FIG. 5. Histograms showing the frequency of specific particles over time (given as frame number) as they enter the second stage of the device after being focused in the first stage using optically mediated hydrodynamic focusing. (a) A mixture of $2.74\text{ }\mu\text{m}$ PS and PMMA particles. (b) A mixture of $2.74\text{ }\mu\text{m}$ PS and $2.39\text{ }\mu\text{m}$ PS particles.

hydrodynamic, and optical coupling interactions that occur in a mound consisting of several hundred particles. We hypothesize that these very complex interactions are significant and become more so as the optical force difference between particles in a sample decreases, but a full treatment of these effects is not the focus of this manuscript. As for the mixtures studied here, using the first stage of the device alone could be effective at separating the 2.74 μm PS and PMMA mixture but would be ineffective for the 2.39 and 2.74 μm PS mixture, thus we developed a second stage method that relies on hydrodynamic focusing to achieve a much finer separation.

IV. CONCLUSIONS

We have shown that the separation capability of our optical chromatography device can be greatly improved by adding a novel hydrodynamic particle focusing region prior to the separation region. This improved design was shown to completely purify and fractionate a mixture of identically sized microparticles with a refractive index difference of only 0.1, which could not be separated in previous work. It was also proposed that by reducing the focused particle band width even more, a further increase in the size based separation capabilities is achievable. The complete fractionation of a sample differing in size by only 350 nm would be a significant achievement and shows the powerful capability of optical chromatography as a separation method.

ACKNOWLEDGMENTS

The authors would like to acknowledge the Office of Naval Research and the Naval Research Laboratory for support of this research.

- ¹D. J. Stevenson, F. Gunn-Moore, and K. Dholakia, *J. Biomed. Opt.* **15**(4), 041503 (2010).
- ²G. Thalhammer, R. Steiger, S. Bernet, and M. Ritsch-Marte, *J. Opt.* **13**(4), 044024 (2011).
- ³R. W. Applegate, D. W. M. Marr, J. Squier, and S. W. Graves, *Opt. Express* **17**(19), 16731–16738 (2009).
- ⁴J. R. Moffitt, Y. R. Chemla, S. B. Smith, and C. Bustamante, *Annu. Rev. Biochem.* **77**, 205–228 (2008).
- ⁵D. G. Grier, *Nature* **424**(6950), 810–816 (2003).
- ⁶C. G. Hebert, A. Terray, and S. J. Hart, *Anal. Chem.* **83**(14), 5666–5672 (2011).
- ⁷A. Ashkin, *IEEE J. Sel. Top. Quant. Electron.* **6**(6), 841–856 (2000).
- ⁸M. P. MacDonald, G. C. Spalding, and K. Dholakia, *Nature* **426**(6965), 421–424 (2003).
- ⁹K. Ladavac, K. Kasza, and D. G. Grier, *Phys. Rev. E* **70**(1), 010901 (2004).
- ¹⁰D. McGloin, G. C. Spalding, H. Melville, W. Sibbett, and K. Dholakia, *Opt. Commun.* **225**(4–6), 215–222 (2003).
- ¹¹R. W. Applegate, Jr., J. Squier, T. Vestad, J. Oakey, D. W. Marr, P. Bado, M. A. Dugan, and A. A. Said, *Lab Chip* **6**(3), 422–426 (2006).
- ¹²J. Oakey, J. Allely, and D. W. M. Marr, *Biotechnol. Prog.* **18**(6), 1439–1442 (2002).
- ¹³T. Imasaka, *Analysis* **26**(5), M53–M55 (1998).
- ¹⁴T. Kaneta, Y. Ishidzu, N. Mishima, and T. Imasaka, *Anal. Chem.* **69**(14), 2701–2710 (1997).
- ¹⁵S. J. Hart, A. Terray, K. L. Kuhn, J. Arnold, and T. A. Leski, *Am. Lab.* **36**(24), 13–17 (2004).
- ¹⁶S. J. Hart and A. V. Terray, *Appl. Phys. Lett.* **83**(25), 5316–5318 (2003).
- ¹⁷S. J. Hart, A. Terray, T. A. Leski, J. Arnold, and R. Stroud, *Anal. Chem.* **78**(9), 3221–3225 (2006).
- ¹⁸A. Terray, J. D. Taylor, and S. J. Hart, *Biomicrofluidics* **3**(4), 044106 (2009).
- ¹⁹S. J. Hart, A. V. Terray, and J. Arnold, *Appl. Phys. Lett.* **91**(17), 171121 (2007).
- ²⁰S. J. Hart, A. Terray, J. Arnold, and T. A. Leski, *Opt. Express* **16**(23), 18782–18789 (2008).
- ²¹X. Su, S. E. Kirkwood, M. Gupta, L. Marquez-Curtis, Y. Qiu, A. Janowska-Wieczorek, W. Rozmus, and Y. Y. Tsui, *Opt. Express* **19**(1), 387–398 (2011).
- ²²I. I. Patel, C. Steuwe, S. Reichelt, and S. Mahajan, *J. Opt.* **15**(9), 094006 (2013).
- ²³A. Mahjoubfar, C. Chen, K. R. Niazi, S. Rabizadeh, and B. Jalali, *Biomed. Opt. Express* **4**(9), 1618–1625 (2013).
- ²⁴J. F. Borowsky, B. C. Giordano, Q. Lu, A. Terray, and G. E. Collins, *Anal. Chem.* **80**(21), 8287–8292 (2008).
- ²⁵A. Terray, H. D. Ladouceur, M. Hammond, and S. J. Hart, *Opt. Express* **17**(3), 2024–2032 (2009).